

Supplementary:

Multi-physical and Electrochemical Coupling Model for the Protonic Ceramic Fuel Cells with $H^+/e^-/O^{2-}$ mixed conducting cathodes

1. Proper constraint expressions for the activation overpotentials and electric boundary settings:

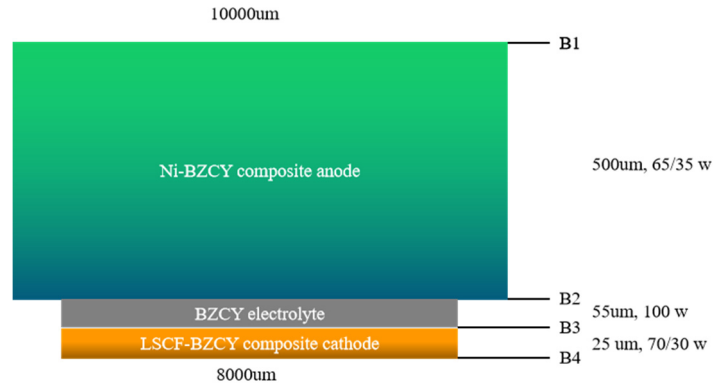
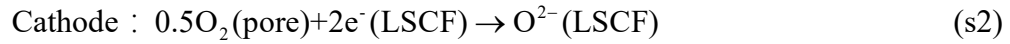
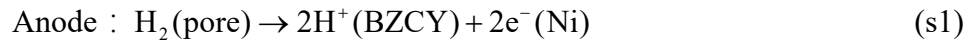


Figure S1. Thickness and material composition of each layer of button cell

Electrochemical reactions in PCFC:



According to the anodic e^- - H^+ charge transfer reaction in Eq. (s1), the electrochemical potentials of the reactants should be balanced at the equilibrium state (no net reaction case), and we have,

$$\mu_{H_2} = 2\mu_{H^+} + 2F\Phi_{H^+}^{\text{eq}} - 2F\Phi_e^{\text{eq}}, [\text{J}]. \quad (\text{s4})$$

$$E_a^{\text{eq}} = \Phi_{H^+}^{\text{eq}} - \Phi_e^{\text{eq}} = \frac{1}{2F}(\mu_{H_2} - 2\mu_{H^+}), [\text{V}]. \quad (\text{s5})$$

where μ_α is the chemical potential of reactant α . It can be evaluated as $\mu_\alpha = \mu_\alpha^{\text{st}} + RT \ln p_\alpha$, where μ_α^{st} is the chemical potential at standard condition ($p^{\text{st}} = 1 \text{ atm}$). T is the local temperature, p_α is the partial pressure of species α at the local reaction sites. F is the Faraday constant, which is the electric content of one mole electrons. $\Phi_{H^+}^{\text{eq}}$ and Φ_e^{eq} are the local equilibrium electrical potentials at the

protonic and electronic conducting phases, respectively. Then the local anode equilibrium electric potential difference E_a^{eq} between two conducting phases can be achieved by Eq. (s6). It is necessary to mention that E_a^{eq} is evaluated based on the working condition instead of the open circuit condition.

For the real operating process with electric current produced, however, the electrochemical potential at the left side of Eq. (s1) should larger than that at the right side,

$$\mu_{\text{H}_2} > 2\mu_{\text{H}^+} + 2F\Phi_{\text{H}^+}^{\text{eq}} - 2F\Phi_e^{\text{eq}}, [\text{J}]. \quad (\text{s6})$$

$$\eta_{\text{act}}^a = E_a^{\text{eq}} - (\Phi_{\text{H}^+} - \Phi_e) = \frac{1}{2F}(\mu_{\text{H}_2} - 2\mu_{\text{H}^+}) - (\Phi_{\text{H}^+} - \Phi_e), [\text{V}]. \quad (\text{s7})$$

In this case, the real local ionic and electronic electric potentials, Φ_{H^+} and Φ_e , should shift from their equilibrium values, $\Phi_{\text{H}^+}^{\text{eq}}$ and Φ_e^{eq} , at equilibrium state. And this shift is defined as the local anode activation overpotential as Eq. (s7).

Generally, for the PEAS located around the percolated Ni-BZCY-pore TPBs, the e^- - H^+ charge transfer rate per unit TPB length j_{TPB}^a (A m^{-1}) can be evaluated as a function of η_{act}^a by the empirical Butler-Volmer equation as,

$$j_{\text{TPB}}^a = j_{\text{TPB},0}^a \left[\exp\left(\frac{2\alpha_f^a F}{RT} \eta_{\text{act}}^a\right) - \exp\left(-\frac{2\beta_r^a F}{RT} \eta_{\text{act}}^a\right) \right], [\text{A m}^{-1}]. \quad (\text{s8})$$

where R is the universal gas constant, α_f^a and β_r^a are the forward and reverse reaction symmetric factors, respectively.

$$j_{\text{TPB},0}^a = j_{\text{TPB},0,\text{ref}}^a \exp\left(-\frac{E_{\text{H}_2}}{R} \left(\frac{1}{T} - \frac{1}{T_{\text{ref}}}\right)\right) \left(\frac{p_{\text{H}_2}}{p_0}\right), [\text{A m}^{-1}] \quad (\text{s9})$$

where E_{H_2} is the activation energy for H_2 oxidation reaction. p_{H_2} is the local hydrogen partial pressure. $j_{\text{TPB},0,\text{ref}}^a$ is assigned empirically at reference temperature T_{ref} .

Similarly, according to the cathode oxygen reduction reaction in Eq. (s2), the equilibrium electrochemical potentials are related as Eq. (s10). Then the cathode equilibrium electric potential difference between electronic and ionic conducting phases can be estimated by Eq. (s11).

$$0.5\mu_{\text{O}_2} - 2F\Phi_e^{\text{eq}} = \mu_{\text{O}_2^-} - 2F\Phi_{\text{O}_2^-}^{\text{eq}}, [\text{J}]. \quad (\text{s10})$$

$$E_c^{eq,1} = \Phi_e^{eq} - \Phi_{O_2}^{eq} = \frac{1}{2F} (0.5\mu_{O_2} - \mu_{O_2}), [\text{V}]. \quad (\text{s11})$$

Once there is output electric current through the cell at working condition, the real local electric potentials, Φ_e and Φ_{O_2} , will shift from their equilibrium values, Φ_e^{eq} and $\Phi_{O_2}^{eq}$. The shift of the local potential difference is defined as the local cathode activation overpotential,

$$\eta_{act}^{c,1} = E_c^{eq,1} - (\Phi_e - \Phi_{O_2}) = \frac{1}{2F} (0.5\mu_{O_2} - \mu_{O_2}) - (\Phi_e - \Phi_{O_2}), [\text{V}]. \quad (\text{s12})$$

For the PEAS located around the percolated LSCF-pore DPBs, the e^- - O^{2-} charge transfer rate per LSCF-particle area can be analogously evaluated as,

$$i_{LSCF} = i_{LSCF,0} \left[\exp\left(\frac{2\alpha_{LSCF}F}{RT} \eta_{act}^{c,1}\right) - \exp\left(-\frac{2\beta_{LSCF}F}{RT} \eta_{act}^{c,1}\right) \right], [\text{A m}^{-2}]. \quad (\text{s13})$$

where α_{LSCF} and β_{LSCF} are the forward and reverse reaction symmetric factors, respectively. The local exchange transfer current based on per unit LSCF-particle area can be obtained as,

$$i_{LSCF,0} = i_{LSCF,0,ref} \exp\left(-\frac{E_{O_2}}{R} \left(\frac{1}{T} - \frac{1}{T_{ref}}\right)\right) \left(\frac{p_{O_2}}{p_0}\right)^{0.25}, [\text{A m}^{-2}]. \quad (\text{s14})$$

where E_{O_2} is the activation energy for O_2 reduction reaction. p_{O_2} is the local oxygen partial pressure. Obviously, the reaction rate is determined by the activity of these potential electrochemical active sites, local oxygen concentration, T , and e^- & O^{2-} electric potentials. $i_{LSCF,0,ref}$ is assigned empirically at reference temperature T_{ref} .

Electrochemical reaction of vapor formation within composite cathode, according to the cathode oxygen reduction reaction in Eq. (s3), the equilibrium electrochemical potentials are related as Eq. (s15). Then the cathode equilibrium electric potential difference between proton and O^{2-} ionic conducting phases can be estimated by Eq. (s16).

$$\mu_{O_2} - 2F\Phi_{O_2}^{eq} + 2\mu_{H^+} + 2F\Phi_{H^+}^{eq} = \mu_{H_2O}, [\text{J}]. \quad (\text{s15})$$

$$E_c^{eq,2} = \Phi_{O_2}^{eq} - \Phi_{H^+}^{eq} = \frac{1}{2F} (\mu_{O_2} + 2\mu_{H^+} - \mu_{H_2O}), [\text{V}]. \quad (\text{s16})$$

Once there is output electric current through the cell at working condition $\mu_{O_2} - 2F\Phi_{O_2}^{eq} + 2\mu_{H^+} + 2F\Phi_{H^+}^{eq} > \mu_{H_2O}$, the real local electric potentials, Φ_{H^+} and Φ_{O_2} , will shift from their equilibrium values, $\Phi_{H^+}^{eq}$ and $\Phi_{O_2}^{eq}$. The shift of the local

potential difference is defined as the local cathode activation overpotential,

$$\eta_{\text{act}}^{\text{c},2} = E_{\text{c}}^{\text{eq},2} - (\Phi_{\text{O}^{2-}} - \Phi_{\text{H}^+}) = \frac{1}{2F} (\mu_{\text{O}^{2-}} + 2\mu_{\text{H}^+} - \mu_{\text{H}_2\text{O}}) - (\Phi_{\text{O}^{2-}} - \Phi_{\text{H}^+}), [\text{V}]. \quad (\text{s17})$$

For the PEAS located around the percolated LSCF-BZCY-pore TPBs, the H^+ - O^{2-} charge transfer rate per LSCF-particle area can be analogously evaluated as,

$$j_{\text{L-B}} = j_{\text{L-B},0} \left[\exp\left(\frac{2\alpha_{\text{f}}^{\text{c}} F}{RT} \eta_{\text{act}}^{\text{c},2}\right) - \exp\left(-\frac{2\beta_{\text{r}}^{\text{c}} F}{RT} \eta_{\text{act}}^{\text{c},2}\right) \right], [\text{A m}^{-2}]. \quad (\text{s18})$$

where $\alpha_{\text{f}}^{\text{c}}$ and $\beta_{\text{r}}^{\text{c}}$ are the forward and reverse reaction symmetric factors, respectively. The local exchange transfer current based on per unit LSCF-particle area can be obtained as,

$$j_{\text{L-B},0} = j_{\text{L-B},0,\text{ref}} \exp\left(-\frac{E_{\text{O-H}}}{R} \left(\frac{1}{T} - \frac{1}{T_{\text{ref}}}\right)\right) \left(\frac{p_{\text{H}_2\text{O}}}{p_0}\right), [\text{A m}^{-2}]. \quad (\text{s19})$$

where $E_{\text{O-H}}$ is the activation energy for generate water vapor reaction. $p_{\text{H}_2\text{O}}$ is the local vapor partial pressure. $j_{\text{L-B},0,\text{ref}}$ is assigned empirically at reference temperature T_{ref} . The working conditions and parameters (i.e., $\alpha_{\text{f}}^{\text{c}}, \beta_{\text{r}}^{\text{c}}, E_{\text{H}_2}, E_{\text{O}_2}, T_{\text{ref}}, p_0, \dots$) are collected in table S2.

Once the properties of each PCFC component layer are assigned, all of the above equations, except for the chemical potentials of oxygen ion $\mu_{\text{O}^{2-}}$ and proton μ_{H^+} in Eqs. (s7), (s12) and (s17), can be resolved by the local independent variables, such as $T, p_{\alpha}, \Phi_{\text{e}}, \Phi_{\text{H}^+}$ and $\Phi_{\text{O}^{2-}}$. For the convenience of solving the Butler Volmer and overpotential equations described above, the local electric potentials, Φ_{H^+} & $\Phi_{\text{O}^{2-}}$, should be shifted by a reference amount to overcome the effects of $\mu_{\text{O}^{2-}}$ and μ_{H^+} . Generally, the constant potential shift does not alter the electronic (or ionic) electric potential profiles within the electronic (or ionic) conducting phase. However, it is very important to note that the relevant overpotential expressions and electric boundary conditions should be changed accordingly to ensure the accuracy of the mathematical model.

$$\hat{\Phi}_{\text{H}^+} = \Phi_{\text{H}^+} + E^{\text{st}} - \frac{1}{2F} (\mu_{\text{H}_2}^{\text{st}} - 2\mu_{\text{H}^+}), [\text{V}]. \quad (\text{s20})$$

$$\hat{\Phi}_{\text{O}^{2-}} = \frac{1}{4F} (\mu_{\text{O}_2}^{\text{st}} - 2\mu_{\text{O}^{2-}}) + \Phi_{\text{O}^{2-}}, [\text{V}]. \quad (\text{s21})$$

In Eq. (s20), E^{st} is added to avoid the appearance of negative value for the proton potential within the anode side.

Then the overpotential expressions in Eqs. (s7), (s12) and (s17) should be respectively rewritten accordingly as,

$$\eta_{act}^a = \frac{1}{2F}(\mu_{H_2} - 2\mu_{H^+}) - (\Phi_{H^+} - \Phi_e) = \Phi_e - \hat{\Phi}_{H^+} + E^{st} + \frac{RT}{2F} \ln \frac{p_{H_2}}{1 \text{ atm}}, [\text{V}]. \quad (\text{s22})$$

$$\eta_{act}^{c,1} = \frac{(\mu_{O_2} - 2\mu_{O^{2-}})}{4F} + \hat{\Phi}_{O^{2-}} - \frac{(\mu_{O_2}^{st} - 2\mu_{O^{2-}})}{4F} - \Phi_e = \hat{\Phi}_{O^{2-}} - \Phi_e + \frac{RT}{4F} \ln \frac{p_{O_2}}{1 \text{ atm}}. \quad (\text{s23})$$

$$\begin{aligned} \eta_{act}^{c,2} &= \frac{1}{2F}(\mu_{O^{2-}} + 2\mu_{H^+} - \mu_{H_2O}) + (\Phi_{H^+} - \Phi_{O^{2-}}) \\ &= \hat{\Phi}_{H^+} - \hat{\Phi}_{O^{2-}} - E^{st} + \frac{1}{2F}(\mu_{H_2}^{st} + 0.5\mu_{O_2}^{st} - \mu_{H_2O}^{st}) + \frac{RT}{2F} \ln \frac{1 \text{ atm}}{p_{H_2O}}, [\text{V}]. \quad (\text{s24}) \\ &= \hat{\Phi}_{H^+} - \hat{\Phi}_{O^{2-}} - \frac{RT}{2F} \ln \frac{p_{H_2O}}{1 \text{ atm}} \end{aligned}$$

where E^{st} is the Nernst potential at the standard state (1 atm). It can be easily calculated as a function of the working temperature T .

As Φ_e in both the anode and cathode sides are not shifted, the cell output voltage V_{op} is kept as the difference between Φ_e at both the cathode/interconnect and anode/interconnect interfaces as,

$$V_{op} = \Phi_e^c|_{B4} - \Phi_e^a|_{B1}, [\text{V}]. \quad (\text{s25})$$

2. Boundary conditions for solving the electrochemical and physical coupling model

The boundary conditions required for all interfaces (indicated in Fig. S1) are analyzed and collected in table S1. B1, B2, B3, B4 represents the anode surface, the connection surface between anode and dense electrolyte, the connection surface between the dense electrolyte and the cathode, the cathode surface, respectively.

Table S1 Boundary condition settings for solving the charge and gas transporting processes

	B1	B2	B3	B4
Electronic charge balance	0	Insulation	Insulation	V_{op}
Proton charge balance	Insulation	Continuity	Continuity	Insulation
Oxygen ionic charge balance			Insulation	Insulation
Mass balance	$c_{H_2}^0 c_{H_2O}^{0,a}$	No Flux	No Flux	$c_{O_2}^0 c_{H_2O}^{0,c} c_{N_2}^0$

The various working parameters simulated and the coefficients used in the governing equations in this model are collected in table S2. Wherein, are the partial pressure of H₂, H₂O at the anode inlet and O₂, H₂O, N₂ at the cathode inlet respectively, which is related to the inlet reactant concentration.

Table S2. working parameters and the coefficients used in the governing equations in this model

Parameters	Value
T_{ref} (K)	1073.15
p_0 (Pa)	1.013×10^5
α_f^a, β_r^a	0.5, 0.5
E_{H_2} (J mol ⁻¹)	100×10^3
$j_{\text{TPB},0,\text{ref}}^a$ (A m ⁻¹)	0.1
$\alpha_{\text{LSCF}}, \beta_{\text{LSCF}}$	0.5, 0.5
E_{O_2} (J mol ⁻¹)	130×10^3
$i_{\text{LSCF},0,\text{ref}}$ (A m ⁻²)	3×10^4
α_f^c, β_r^c	0.5, 0.5
$j_{\text{L-B},0,\text{ref}}$ (A m ⁻¹)	0.2
$E_{\text{O-H}}$ (J mol ⁻¹)	20×10^3
$p_{\text{H}_2}^0, p_{\text{H}_2\text{O}}^{0,\text{a}}$ (atm)	0.97, 0.03
$p_{\text{O}_2}^0, p_{\text{H}_2\text{O}}^{0,\text{c}}, p_{\text{N}_2}^0$ (atm)	0.21, 0.07, 0.79

3. The effect of the microstructure parameters on the PCFC performance

Figs. S2a, S2b and S2c show the dependences of the local oxygen ions and protons generation rates distributions on different ratio of LSCF/BZCY (7/3 5/5 3/7), and porosities, respectively.

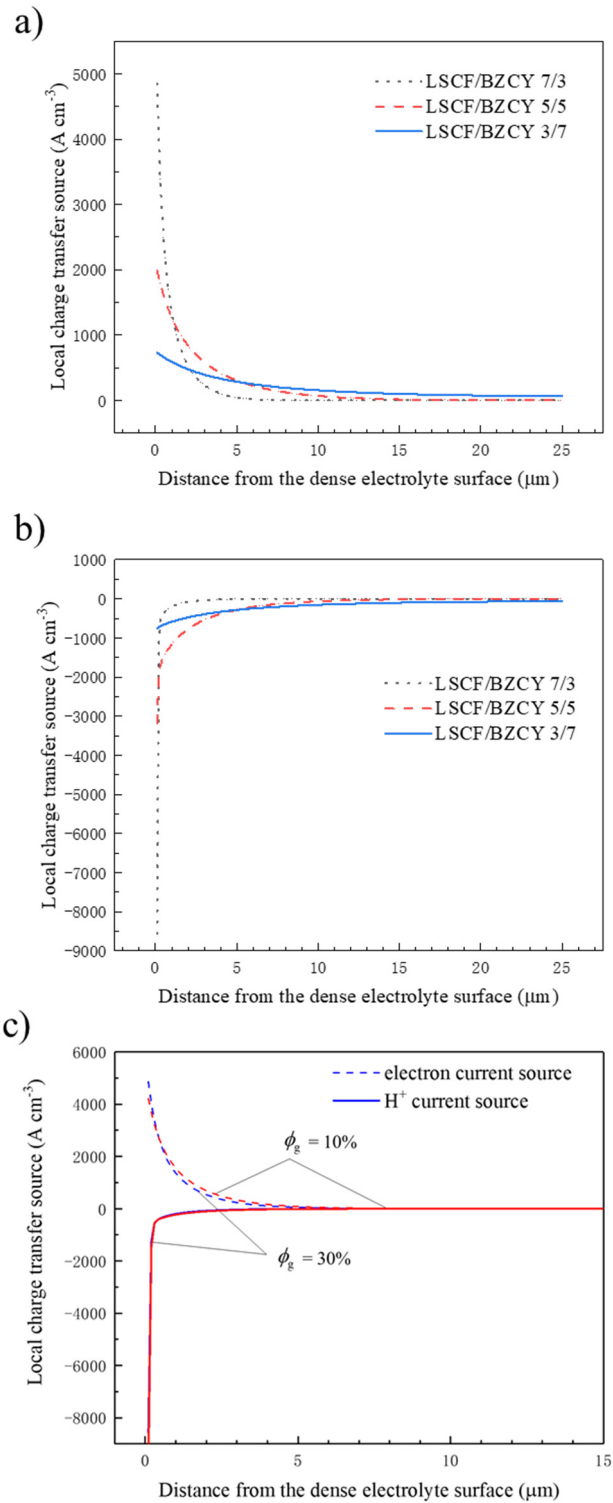


Figure S2. The dependences of the distributions of the local electronic and protons consumption rates on different ratio of LSCF:BZCY, and different porosity in cathode. **(a)** electronic charge transfer source; **(b)** protons transfer source. **(c)** different porosity of cathode.

In Figs. S3, the effect of different particle radii on the distributions of the local electronic and protons consumption rates, and the PCFC performance are displayed, respectively.

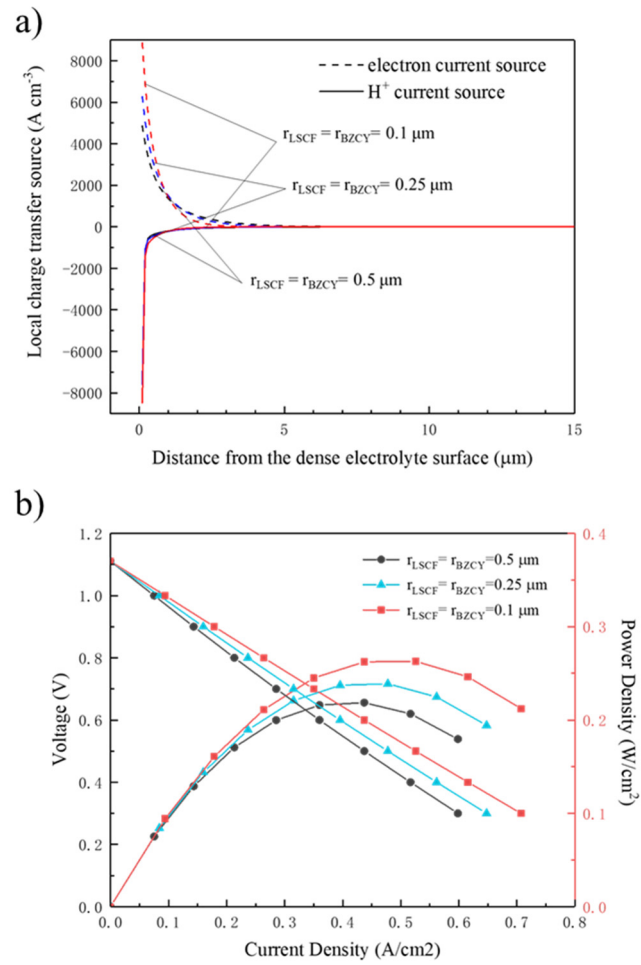


Figure S3. The effect of different particle radii on: (a) the distributions of the local electronic and protons consumption rates; (b) PCFC performance.